Journal of Molecular Pathophysiology
www.scopemed.org
DOI: 10.5455/jmp.20141122032817

Original Research

GESDAV

Disulfiram neurotoxicity: Decrements in ethanolamine, serine, and inositol glycerophospholipids

Paul L. Wood, Ryan S. Alexander, Cameron C. Felty

Department of Physiology and Pharmacology, DeBusk College of Osteopathic Medicine, Lincoln Memorial University, 6965 Cumberland Gap Pkwy., Harrogate, TN 37752, USA

Address for correspondence:
Paul L. Wood, Department of Physiology and Pharmacology, DeBusk College of Osteopathic Medicine, Lincoln Memorial University, 6965 Cumberland Gap Pkwy., Harrogate, TN 37752, USA. E-mail: paul.wood@lmunet.edu

Received: November 20, 2014
Accepted: November 22, 2014
Published: December 11, 2014

ABSTRACT

Aim: Disulfiram has rare serious neurotoxicities including optic neuropathy, peripheral neuropathy and basal ganglia lesions. Since the mechanism of these toxicities is not understood, we undertook a lipidomics analysis of the effects of disulfiram on human lymphoblasts. **Materials and Methods:** Human lymphoblasts were incubated with disulfiram, and the cellular lipidome was analyzed by ESI-high resolution mass spectrometry. **Results:** Disulfiram decreased the levels of a large number of glycerophospholipids, sphingolipids, and diacylglycerols. **Conclusion:** Disulfiram has dramatic effects on the levels of structural lipids in human lymphoblasts. These actions may explain the neurotoxicities of this drug in humans.

KEY WORDS: Disulfiram, lipidomics, lymphoblasts, neurotoxicity

INTRODUCTION

Disulfiram (antabuse), an inhibitor of acetaldehyde dehydrogenase, is a drug used extensively in the treatment of alcohol addiction. This drug is generally safe but does have some rare, serious adverse effects. The most serious of these side-effects are various neurotoxicities including optic neuropathy, peripheral neuropathy, and white matter damage in the basal ganglia resulting in dystonia and akinesia. These toxicities generally occur with long-term dosing [1-3], in over-dose situations [4], and are irreversible in some cases. However, they can also occur with short dosing periods of several weeks in some individuals [5-6].

Efforts to study the mechanisms of these neurotoxicities are complicated by the many metabolites of disulfiram [7]. The predominant hypothesis is that metabolites of disulfiram induce oxidative stress resulting in demyelination; however, animal studies do not support this hypothesis [8]. We therefore decided to examine the effects of disulfiram on human lymphoblasts which are useful for studying human lipid pathways [9] and undertook a shotgun lipidomics analysis [10]utilizing an analytical platform that measures of over 900 individual lipids across 27 lipid subfamilies [11-14].

MATERIALS AND METHODS

Tissue Culture

Human lymphoblasts (GM07210, Coriell Cell Repositories) were grown as suspension cultures in 12 well plates with HyClone RPMI-1640 medium containing 10% fetal bovine serum, 25 mM HEPES, 2 mM glutamine, and 100 μg/ml penicillin/ streptomycin in an incubator at 37°C and 5% CO_2. Lymphoblasts were incubated with disulfiram dissolved in dimethyl sulfoxide (DMSO) such that the final DMSO concentration was 0.1%. For lipid replacement experiments, krill oil (Now Foods, Neptune krill oil) was dissolved in ethanol such that the final ethanol concentration was 0.1%. Cells were harvested by centrifugation at 4,500 × g for 10 min with the cell pellet washed once with cold phosphate-buffered saline.

Lipid Extraction and Analysis

Lipids were extracted with methy-tert-butyl ether and methanol containing [$^2H_8$]arachidonic acid, [$^2H_4$]hexacosanoic acid, [$^{13}C_{18}$]stearic acid, [$^2H_{28}$]DC 16:0, [$^2H_7$]cholesterol sulfate, [$^2H_5$]MAG 18:1, [$^{13}C_3$]DG 36:2, [$^2H_5$]TAG 48:0, [$^2H_{31}$]PtdE 34:1, [$^2H_{54}$]PtdE 28:0, [$^2H_{31}$]PtdC 34:1, [$^2H_{54}$]PtdC 28:0, [$^2H_{62}$] PtdC 32:0, [$^2H_{31}$]SM 16:0, [$^2H_{31}$]PS 36:1, [$^2H_{31}$]PA 34:1, [$^2H_{62}$] PG 32:0, [$^2H_3$]carnitine 18:0, [$^2H_4$]LPC, CL(56:0), glyburide, and bromocriptine as internal standards. Extracts were dried by centrifugal vacuum evaporation and dissolved in isopropanol: methanol: chloroform (4:2:1) containing 15 mM ammonium acetate. Shotgun lipidomics (5 μL per min) were performed utilizing high-resolution (140,000 at 200 amu) data acquisition, with sub-millimass accuracy on an orbitrap mass spectrometer (Thermo Q Exactive) with successive switching between polarity modes [10-12]. Washes (500 μL) with methanol followed by hexane/ethyl acetate (3:2), between samples, were used to minimize ghost effects.

In negative ion ESI, the anions of ethanolamine plasmalogens (PlsE), phosphatidylethanolamines (PtdE), lysophosphatidylethanolamines (LPE), lysoalkenyl-acyl glycerophosphoethanolamines (LPEp), phosphatidylglycerols (PG), lysophosphatidylglycerols (LPG), phosphatidic acids, lysophosphatidic acids, phosphatidylinositols (PI), lysoph ospatidylinositols, phosphatidylserines (PS), lysophospha tidylserines, ceramides (Cer), N-acylphosphatidylserines, N-acyl serines, fatty acids, dicarboxylic acids, very-long-chain fatty acids, and sulfatides (Sulf), and the $[M-2H]^{2-}$ anions of cardiolipins were quantitated and lipid identities validated by MS/MS with high resolution analyses of products.

In positive ion ESI, the cations of choline plasmalogens (PlsC), phosphatidylcholines (PtdC), lysophosphatidylcholines (LPC), sphingomyelins (SM), sphingosine, monoacylglycerols (MG), platelet-activating factors, acylcarnitines, Cer, and the ammonium adducts of diacylglycerols (DG), triacylglycerols (TG), and cholesterol esters were quantitated and lipid identities validated by MS/MS with high resolution analyses of product ions. The cations and anions of bromocriptine and glyburide were used to monitor for potential mass axis drift.

Statistical Analysis

R-values (ratio of endogenous lipid peak area to the peak area of an appropriate internal standard), corrected for protein, were calculated. In the cases where percent of control is presented, the calculations were % of control = ([Tx mean]/[control mean] [1 ± SQRT[Tx standard deviation [SD]/Tx mean]]^2 + [control SD/control mean]^2). Proteins were determined utilizing the Pierce bicinchoninic acid protein assay kit (Thermo Fisher). Data are presented as mean ± SD. A one-way ANOVA with 95% confidence level was used to determine significant differences within the data. The Tukey-Kramer was used as a *post-hoc* test to compare all the groups to one another.

RESULTS

Disulfiram Concentration-response

Disulfiram decreased the cellular levels of ethanolamine glycerophospholipids in a concentration-dependent manner (10, 100, and 500 μM) after a 24 h incubation [Figure 1]. These included PtdE, PlsE, and LPE. Choline glycerophospholipids were much less affected by disulfiram treatment [Figure 2]. PI, PS, and PG were decreased after disulfiram treatment [Figure 3]. The sphingolipids, sphingomyelin, and Sulf also were decreased while ceramide levels were unaltered in disulfiram-treated cells [Figure 4]. Very-long-chain dicarboxylic acids [Figure 3] and DG [Figure 4]also were decreased, while increases in monoacylglycerol [Figure 5]and TG [Figures 3 and 5] were noted.

Disulfiram Time-response

Disulfiram produced time-dependent decreases in glycerophospholipid pools with maximal decrements occurring at 48 h [Figure 5].

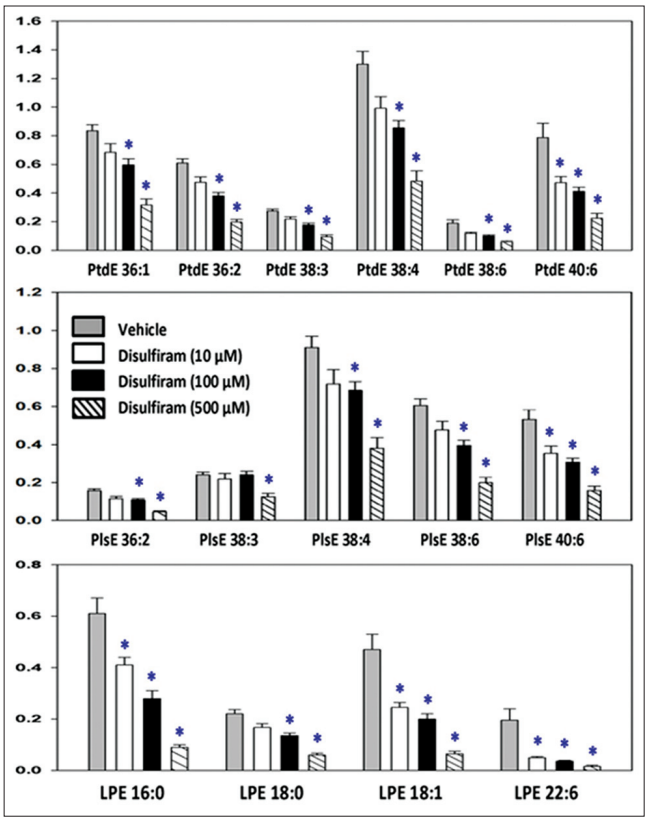

Figure 1: Lymphoblast levels of phosphatidylethanolamines, ethanolamine plasmalogens, and lysophosphatidylethanolamines 24 h. after addition of 10, 100, or 500 µM disulfiram. Y axis is the ratio of the peak area of the endogenous lipid to the peak area of a stable isotope internal standard, corrected for cellular protein. The data are presented as mean ± standard deviation for 12 tissue culture wells. *, $P < 0.05$ versus vehicle control

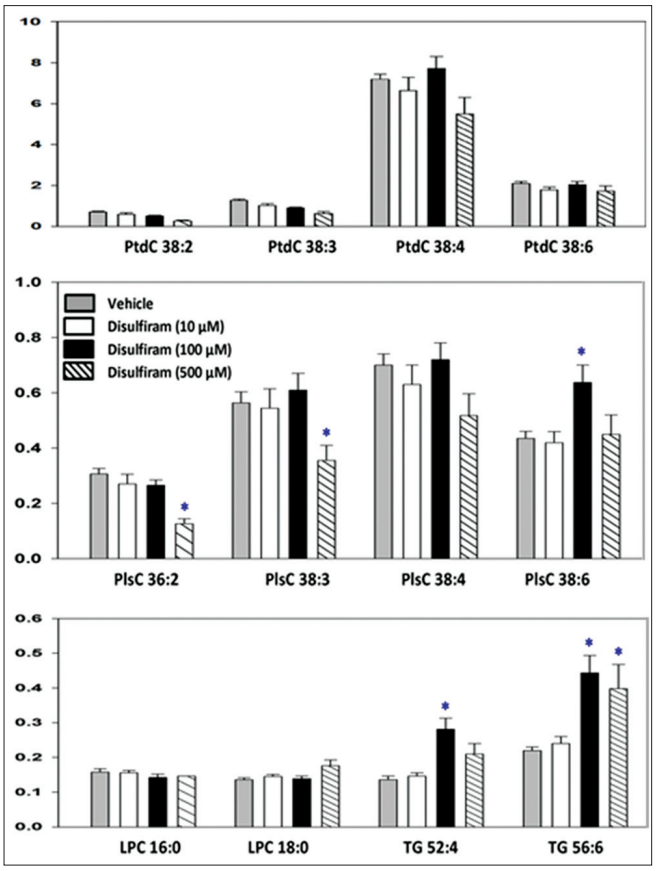

Figure 2: Lymphoblast levels of phosphatidylcholines, choline plasmalogens, lysophosphatidylcholines, and triacylglycerols 24 h. after addition of 10, 100, or 500 µM disulfiram. Y axis is the ratio of the peak area of the endogenous lipid to the peak area of a stable isotope internal standard, corrected for cellular protein. The data are presented as mean ± standard deviation for 12 tissue culture wells. *, $P < 0.05$ versus vehicle control

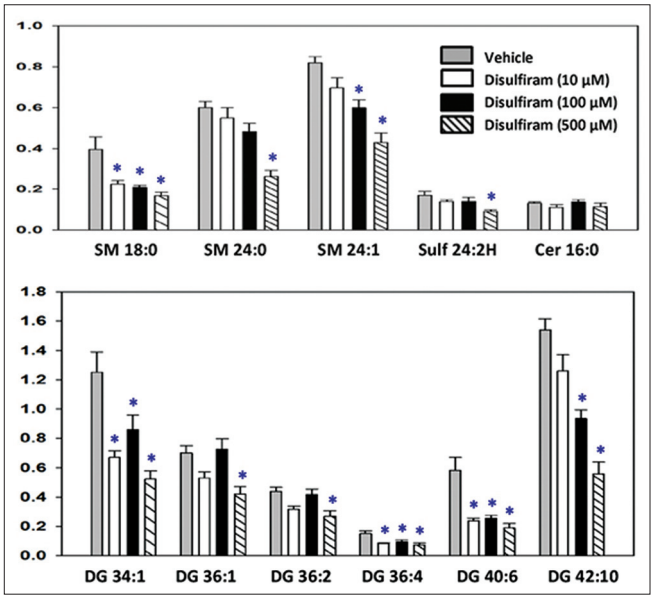

Figure 3: Lymphoblast levels of phosphatidylinositols, phosphatidylserines, phosphatidylglycerols, and very-long-chain dicarboxylic acids 24 h. after addition of 10, 100, or 500 µM disulfiram. Y axis is the ratio of the peak area of the endogenous lipid to the peak area of a stable isotope internal standard, corrected for cellular protein. The data are presented as mean ± standard deviation for 12 tissue culture wells. *, $P < 0.05$ versus vehicle control

Lipid Replacement Strategy: Krill Oil

Incubation of disulfiram-treated cells with krill oil resulted in augmentation of ethanolamine glycerophospholipids but not PI, PS, or PG [Figure 6].

DISCUSSION

Disulfiram is an important drug in the treatment of alcohol abuse and is under clinical evaluations in a number of other addictions [15]. However, a number of serious neurotoxicities can develop with this drug [1-6]. Our data are the first to demonstrate that these neurotoxicties involve dramatic decrements in critical structural glycerophospholipids and sphingolipids. The large dose- and time-dependent decreases in membrane diacyl-glycerophospholipids are complicated in that PtdE, PS, PI, and PG levels are lowered while PtdC levels are unaffected. Since these lipids have common precursor molecules [Figure 7], it is most likely that the metabolism of the affected lipids is occurring at a more rapid rate than synthesis can keep pace with. The demands on synthesis are further validated by our observations of decreased levels of DG, precursors to

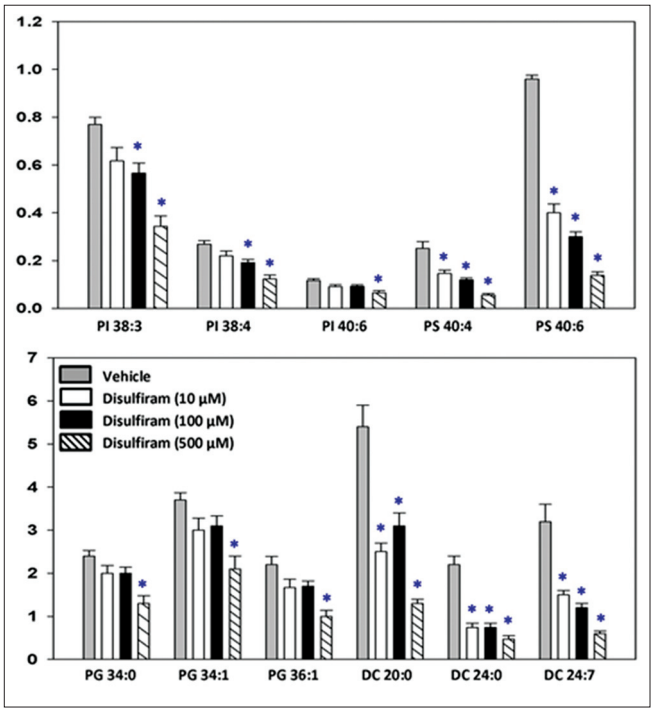

Figure 4: Lymphoblast levels of sphingomyelins, sulfatides, ceramides, and diacylglycerols 24 h. after addition of 10, 100, or 500 µM disulfiram. Y axis is the ratio of the peak area of the endogenous lipid to the peak area of a stable isotope internal standard, corrected for cellular protein. The data are presented as mean ± standard deviation for 12 tissue culture wells. *, $P < 0.05$ versus vehicle control

glycerophospholipids [Figure 7]. Furthermore, the observed increases in MG suggest that acylation of MG to DG may be

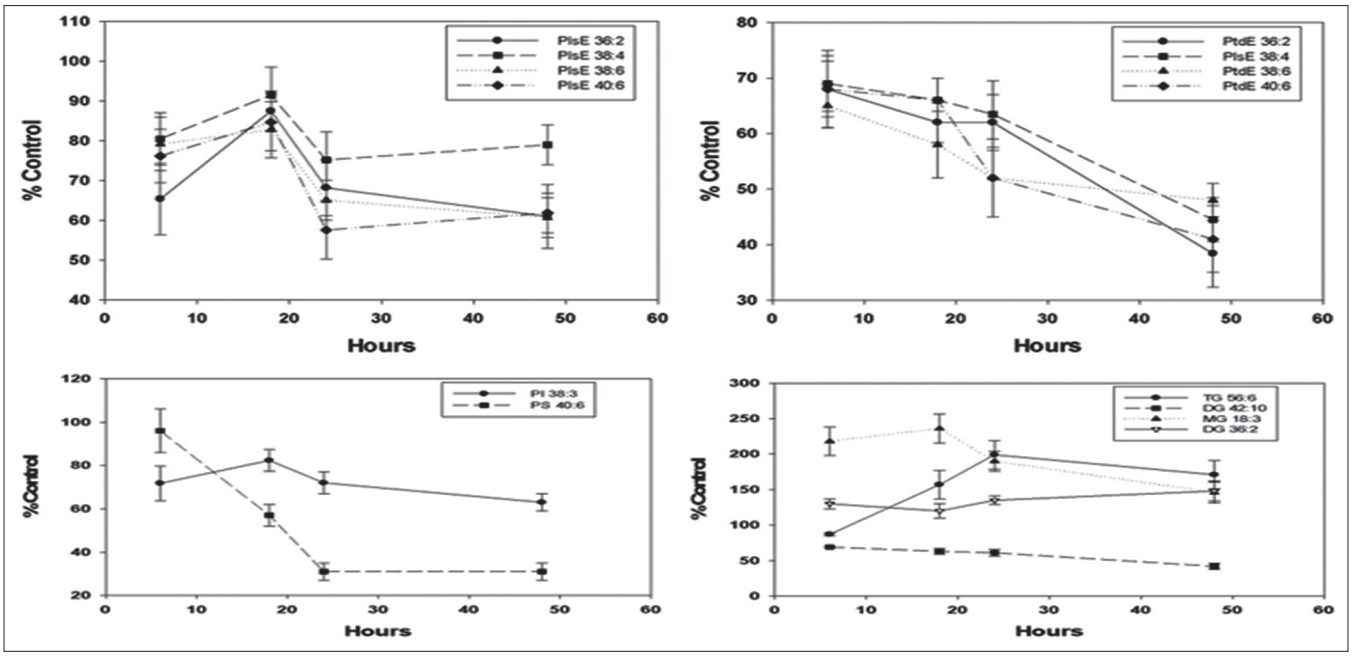

Figure 5: Time course for the effects of disulfiram (100 μM) on lymphoblast levels of phosphatidylethanolamines, ethanolamine plasmalogens, phosphatidylinositols, phosphatidylserines, triacylglycerols, monoacylglycerols, and diacylglycerols. The data are presented as mean ± standard deviation for 6 tissue culture wells. *, $P < 0.05$ versus vehicle control

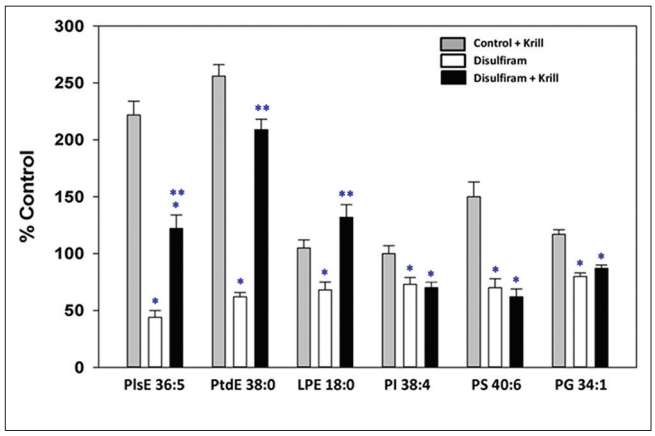

Figure 6: Lymphoblast levels of ethanolamine plasmalogens, phosphatidylethanolamines, lysophosphatidylethanolamines, phosphatidylinositols, phosphatidylserines, and phosphatidylglycerols after a 12 h. incubation with 100 μM disulfiram or vehicle followed by a further 18 h. incubation with kr ill oil (200 μg/well). Cells were washed once with fresh media between treatments. The data are presented as mean ± standard deviation for 6 tissue culture wells. *, $P < 0.05$ versus vehicle control; **, $P < 0.05$ versus disulfiram + vehicle

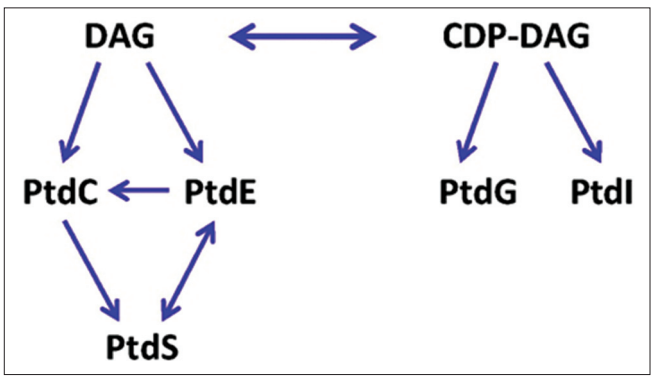

Figure 7: Biosynthetic pathways of glycerophospholipids from the diacylglycerol pool. cytidine diphosphate; diacylglycerol, phosphatidylcholines, phosphatidylethanolamines, phosphatidylglycerol, phosophatidylinositol, phosphatidylserine

inhibited by disulfiram, in addition to inhibition of degradation of the MG pool by MG lipase [16]. The DG pool, in addition to supplying precursors for structural glycerophospholipids and TG, also function as signal transduction mediators and are essential structural lipids of the nuclear envelope and nucleoplasmic reticulum [17,18]. Therefore, it is prudent to also speculate that DG-dependent alterations in nuclear function may contribute to the toxicity of disulfiram.

The decrements that we noted in lysophosphoethanolamines further support the suggestion of augmented glycerophospholipid degradation. Maintenance of PtdC levels may involve decreased degradation along with decreased base exchange to generate PS [19]and by increased methylation of PtdE to maintain the PtdC pool [20]. Our experiments with krill oil, which contains a large variety of glycerophosphocholines, glycerophosphoethanolamines, and their precursors [21], further demonstrate that synthetic pathways are intact and can be augmented with metabolic precursors.

Plasmalogens, another class of critical membrane lipids [22], also were decreased in the case of PlsE but not PlsC. These data suggest that PlsE may be utilized to support choline plasmalogen levels. The biosynthesis of very-long-chain dicarboxylic acids involves the ω-oxidation of very-long-chain fatty acids. This is a complicated pathway involving fatty aldehyde dehydrogenase an enzyme inhibited by disulfiram [23-25]. Our data also

demonstrate that disulfiram is a potent inhibitor of fatty aldehyde dehydrogenase in that we monitored dramatic reductions in very-long-chain dicarboxylic acids. In addition, since fatty aldehyde dehydrogenase metabolizes fatty aldehydes generated during plasmalogen metabolism [26], accumulation of these reactive aldehydes could lead to cytotoxicity [27].

In the case of structural sphingolipids, large decreases in the levels of SM were measured while Sulf and Cer were minimally affected by disulfiram. Since the ceramide pool provides precursors for both SM and Sulf, these data also suggest that the enhanced metabolism of SM is responsible for the decrements in these sphingolipids.

CONCLUSION

We observed dramatic decrements in structural lipids after treatment of human lymphoblasts with disulfiram. Our data suggest that catabolic pathways are activated and that this mechanism may be responsible for the clinical neurotoxicities of disulfiram.

ACKOWLEDGMENTS

This research was funded by Lincoln Memorial University, DeBusk College of Osteopathic medicine (LMU-DCOM). RSA and CCF received summer medical student awards from LMU-DCOM.

REFERENCES

1. Boukriche Y, Weisser I, Aubert P, Masson C. MRI findings in a case of late onset disulfiram-induced neurotoxicity. J Neurol 2000;247:714-5.
2. Borrett D, Ashby P, Bilbao J, Carlen P. Reversible, late-onset disulfiram-induced neuropathy and encephalopathy. Ann Neurol 1985;17:396-9.
3. Krauss JK, Mohadjer M, Wakhloo AK, Mundinger F. Dystonia and akinesia due to pallidoputaminal lesions after disulfiram intoxication. Mov Disord 1991;6:166-70.
4. Laplane D, Attal N, Sauron B, de Billy A, Dubois B. Lesions of basal ganglia due to disulfiram neurotoxicity. J Neurol Neurosurg Psychiatry 1992;55:925-9.
5. Kulkarni RR, Pradeep AV, Bairy BK. Disulfiram-induced combined irreversible anterior ischemic optic neuropathy and reversible peripheral neuropathy: A prospective case report and review of the literature. J Neuropsychiatry Clin Neurosci 2013;25:339-42.
6. Zorzon M, Masè G, Biasutti E, Vitrani B, Cazzato G. Acute encephalopathy and polyneuropathy after disulfiram intoxication. Alcohol Alcohol 1995;30:629-31.
7. Johansson B. A review of the pharmacokinetics and pharmacodynamics of disulfiram and its metabolites. Acta Psychiatr Scand Suppl 1992;369:15-26.
8. Tonkin EG, Valentine HL, Zimmerman LJ, Valentine WM. Parenteral N,N-diethyldithiocarbamate produces segmental demyelination in the rat that is not dependent on cysteine carbamylation. Toxicol Appl Pharmacol 2003;189:139-50.
9. Wood PL, Khan MA, Smith T, Ehrmantraut G, Jin W, Cui W, *et al. In vitro* and *in vivo* plasmalogen replacement evaluations in rhizomelic chrondrodysplasia punctata and Pelizaeus-Merzbacher disease using PPI-1011, an ether lipid plasmalogen precursor. Lipids Health Dis 2011;10:182.
10. Wood PL. Mass spectrometry strategies for clinical metabolomics and lipidomics in psychiatry, neurology, and neuro-oncology. Neuropsychopharmacology 2014;39:24-33.
11. Wood PL, Shirley NR. Lipidomics analysis of postmortem interval: Preliminary evaluation of human skeletal muscle. Metabolomics 2013;3:3.
12. Wood, PL, Phillipps, A, Woltjer, RL, Kaye, JA, Quinn, JF. Increased lysophosphatidylethanolamine and diacylglycerol levels in Alzheimer's disease plasma. JSM Alzheimer's Dis Relat Dementia 2014;1:1001.
13. Wood PL. Accumulation of N-acylphosphatidylserines and N-acylserines in the frontal cortex in schizophrenia. Neurotransmitter 2014;1:e263.
14. Wood PL, Bravermann NE. Lipidomics analysis of peroxisomal disorders: Discovery of deficits in phosphatidyglycerol levels in rhizomelic chondrodysplasia type 1. J Data Mining Genomics Proteomics 2014;S1:001.
15. Douaihy AB, Kelly TM, Sullivan C. Medications for substance use disorders. Soc Work Public Health 2013;28:264-78.
16. Labar G, Bauvois C, Muccioli GG, Wouters J, Lambert DM. Disulfiram is an inhibitor of human purified monoacylglycerol lipase, the enzyme regulating 2-arachidonoylglycerol signaling. Chembiochem 2007;8:1293-7.
17. Peddie CJ, Blight K, Wilson E, Melia C, Marrison J, Carzaniga R, *et al.* Correlative and integrated light and electron microscopy of in-resin GFP fluorescence, used to localise diacylglycerol in mammalian cells. Ultramicroscopy 2014;143:3-14.
18. Domart MC, Hobday TM, Peddie CJ, Chung GH, Wang A, Yeh K, *et al.* Acute manipulation of diacylglycerol reveals roles in nuclear envelope assembly & endoplasmic reticulum morphology. PLoS One 2012;7:e51150.
19. Tomohiro S, Kawaguti A, Kawabe Y, Kitada S, Kuge O. Purification and characterization of human phosphatidylserine synthases 1 and 2. Biochem J 2009;418:421-9.
20. Vance DE. Phospholipid methylation in mammals: From biochemistry to physiological function. Biochim Biophys Acta 2014;1838:1477-87.
21. Winther B, Hoem N, Berge K, Reubsaet L. Elucidation of phosphatidylcholine composition in krill oil extracted from Euphausia superba. Lipids 2011;46:25-36.
22. Wood PL. Lipidomics of Alzheimer's disease: Current status. Alzheimers Res Ther 2012;4:5.
23. Zorzano A, Herrera E. Differences in the kinetic properties and sensitivity to inhibitors of human placental, erythrocyte, and major hepatic aldehyde dehydrogenase isoenzymes. Biochem Pharmacol 1990;39:873-8.
24. Zorzano A, Herrera E. Differences in kinetic characteristics and in sensitivity to inhibitors between human and rat liver alcohol dehydrogenase and aldehyde dehydrogenase. Gen Pharmacol 1990;21:697-702.
25. Sanders RJ, Ofman R, Dacremont G, Wanders RJ, Kemp S. Characterization of the human omega-oxidation pathway for omega-hydroxy-very-long-chain fatty acids. FASEB J 2008;22:2064-71.
26. Rizzo WB. Fatty aldehyde and fatty alcohol metabolism: Review and importance for epidermal structure and function. Biochim Biophys Acta 2014;1841:377-89.
27. Wood PL, Khan MA, Moskal JR. The concept of "aldehyde load" in neurodegenerative mechanisms: Cytotoxicity of the polyamine degradation products hydrogen peroxide, acrolein, 3-aminopropanal, 3-acetamidopropanal and 4-aminobutanal in a retinal ganglion cell line. Brain Res 2007;1145:150-6.

Source of Support: Nil, Conflict of Interest: None declared.